

RECENT SEISMOLOGICAL PROJECTS AND SEISMIC INVESTIGATIONS OF THE CRUST AND UPPER MANTLE STRUCTURE OF THE CASPIAN BASIN.

McBride John, Bullard Labs, Department of Earth Sciences, Cambridge University, United Kingdom

Priestley, Keith, Bullard Labs, Department of Earth Sciences, Cambridge University, United Kingdom.

Rozhkov Mikhail, SYNAPSE Science Center / Moscow IRIS Data Analysis Center, Russia.

The paper reflects the state of recent joint international seismological researches of the Caspian Sea Basin, and first results, achieved during deploying the **Caspian Seismic Network (CSN)**. Being one of the main instrument for studying the Earth deep structure, modern seismological techniques are based upon new data, collected with the help of modern technologies of data acquisition. Present seismic installations of the Caspian Basin, jointly operated by scientists from different countries, highly satisfy such concept. Two major passive experiments must be mentioned here: (1) joint Russian-British program **CSN** on studying **South Caspian Basin** structure conducted by the **University of Cambridge (UC)**, UK, and **SYNAPSE Science Center (SSC)**, Russia, and (2) small aperture array (**IRIS SAA**) program conducted by the **Incorporated Research Institutions for Seismology of the United States (IRIS)**. Both programs are being performed with the technical support of the Institute of Seismology of Turkmenian Academy of Sciences. Program (2) was mainly performed by the University of California San Diego during past 2 years. Huge amount of data, recorded by more than 50 instruments of "seismic antenna" nearby the city of Ashgabad, soon will be available for the scientific community through the **IRIS Data Management System** (if you are Internet user, check <http://www.iris.washington.edu>). In current paper we would like to describe progress made within the framework of **CSN** program.

Tectonic Environment. The Caspian Sea sits astride the greater Alpine-Himalayan foldbelt within the south-central part of the former USSR in central Asia (locally the Great Caucasus-Kopet Dagh fold and thrust belt). Knowledge of the seismic velocity structure of the crust and upper mantle beneath the Caspian Sea will add considerably to our understanding of the development of mountain building arising from convergence of the Gondwanaland supercontinent and Eurasia in a poorly understood region that could be thought of as transitional between the Alps and the Himalayas. Neogene calc-alkaline volcanism and active seismicity along the Great Caucasus and the Alborz mountains suggest geologically recent and possibly current subduction. A major geodynamic question is how can the margin of a major Alpine foldbelt be locally submerged beneath more than 20 km of sediment that have collected in an immense hollow known as the south Caspian Basin. This area, which is subsiding so rapidly that it is below sea level, is floored by 'ocean-like' crust that has had several explanations put forward based on broad seismic velocity patterns but without any knowledge of detailed deep structure.

Fig.1

A tectonic model for the Iran - south Caspian Sea region was proposed by McKenzie (1972) and has been further developed in subsequent studies (e.g., Jackson and McKenzie, 1984; Baker et al, 1993; Baker, 1993; Priestley et al, 1994). The region consists of two relatively aseismic blocks surrounded by zones of high seismicity. The southern block consists of the plateau of central Iran which is moving northward as a semi-rigid block. Along the northern border of Iran, in the Alborz and Kopet Dagh mountains, the overall direction of motion is toward the NE.

The south Caspian basin and the Turkmenian Lowlands form an anomalous aseismic depression that is bounded to the north by the Apsheron-Balkhan Sill, a narrow seismogenic zone extending from the Caucasus Mountains in Azerbaijan to the Kopet Dagh Mountains of Turkmenistan; and to the west in Azerbaijan and to the south along the Iranian border by the active fold and thrust belts of the Talesh and Alborz Mountains, respectively. The northward movement of the Iranian plate with respect to the Eurasian plate is causing compressional deformation throughout the Caspian region. Mechanisms of earthquakes occurring within these bounding seismic belts suggest that the suspected "ocean-like" crust of the south Caspian basin, is being overridden by the continental crust of the Iranian plateau in the south, and to a lesser extent, by northern Caspian continental crust.

Crust and Upper Mantle Structure. There have been several studies focused on the crust and upper mantle structure of the Middle East; however, in contrast to the tectonics, the seismic velocity structure of Iran and the south Caspian basin remains only poorly known. There are significant differences in the results of these studies. For example, the Pn velocity for Iran has been determined in four studies. Chen et al (1980) estimates Pn velocity from regional earthquakes recorded at the nearby WWSSN stations **MSH** and **TAB** to be 8.02 +/- 0.07 km/s and 7.85 +/- 0.05 km/s, respectively. Using similar data, Kadinsky-Cade et al (1981) have shown that the **Pn** velocity varies significantly as a function of azimuth at station **TAB** (7.6 +/- 0.5 km/s to 8.6 +/- 0.5 km/s). Some of the discrepancy in these two studies may arise from the poor earthquake locations determined for events in the Middle East (Asudeh, 1983). Both Kadinsky-Cade et al (1981) and Hearn and Ni (1994) found the Pn velocity beneath the southern Caspian basin to be about 8.0 km/s.

The velocity structure of the south Caspian basin is also poorly known. Deep seismic sounding data collected in the early 1960's suggests that the crust of the south Caspian basin and west Turkmenian Lowlands consists of 2 layers; a thick sedimentary layer (15-20 km) with a P-wave velocity of 3.5-4.0 km/s which overlies a 12-18 km thick "basaltic" layer with a P-wave velocity of 6.6-7.0 km/s (Neprochnov 1968; Rezanov and Chamo, 1969). It has been suggested that the south Caspian basin represents a section of "ocean-like" crust that may be either a relic of an older Paleozoic-Triassic ocean, or a marginal sea which developed behind a Mesozoic-Paleogene ocean (Berberian and King 1981; Berberian 1983).

Regional phase propagation characteristics of **Sn** across the Iranian plateau, the Caspian Sea and surrounding regions have been discussed in several studies. Zones of inefficient **Sn** propagation are identified beneath the Alborz Mountains just south of the Caspian Sea, as well as beneath NE Iran and NW Afghanistan (Kadinsky-Cade et al, 1981; Molnar and Oliver 1969). Efficient **Sn** propagation has been reported beneath the southern Caspian basin which supports the ocean-like crustal hypothesis discussed earlier (Kadinsky-Cade et al, 1981; Wallace et al, 1992).

The amplitude decay characteristics across the Iranian plateau are discussed in moderate detail in three previous works. Jih and Lyness (1992) and Nuttli (1981) constrained the attenuation parameters γ and **Q** derived from **Lg** and characterize the Iranian plateau in general as a region of low **Q** (<250), although the distinction between absorption and scattering remains obscure. Wallace et al, (1992) observes inefficient **Lg** propagation across northern Iran and the southern Caspian region. For travel paths across the southern Caspian region, the **Lg** phase is scattered or blocked (Kadinsky-Cade et al 1981). Using data from our recently installed seismograph network discussed below, we have observed that both the shorter and longer period surface wave train is strongly attenuated or scattered within the southern Caspian basin. In addition to lateral variations in crustal structure, changes in topography have recently been shown to affect Lg propagation. Recent analysis of the logarithmic rms amplitude ratio of Sn/Lg (Zhang and Lay 1994) has shown that this ratio can be linearly related to changes in surface

topography. We are using the teleseismic body wave data to determine single station receiver functions which are interpreted in terms of the shear wave velocity structure beneath each site. We are also measuring surface wave phase velocity dispersion between the sites to determine the lithospheric velocity structure of the south Caspian basin.

CASPIAN SEISMIC NETWORK. CSN research project was started for better understanding of the seismic structure of the south Caspian Basin and the surrounding region. There are two main goals of this experiment: (1) to better define the complex crust and upper mantle structure in the area; and (2) to better understand regional seismic wave propagation in the region. To accomplish this we have installed a number of broad-band digital recording seismographs around the Caspian and operated these for about two years. Data at each CSN station is recorded on a **Refraction Technology 72a-02 data loggers** which are equipped with either **Omega** or **GPS** timing, an external hard disks and a **Guralp CMG-3T triaxial broadband feedback seismometers**. The Turkmenian stations **KRV** (Krasnavodsk), **NBD** (Nebit-Dag), **DTA** (Dana-Ata), **KAT** (Kyzyl-Atrek) and recently installed **KRL** (Kara-Kala) are operated in cooperation with Dr. B. Karryev from the Institute of Seismology of Turkmenistan. In Azerbaijan the stations **LNK** (Lenkoran) and **BAK** (Baku), later moved to Shemakha (**SHE**), were operated in cooperation with Dr. S. Agamirzoev from the Geophysical Expedition of Azerbaijan. (**Fig.2 Stations location**) Last spring Azerbaijanian part of the program was terminated due to political situation at this region. In addition to the data from our seismograph network, this study incorporates data from the IRIS seismograph station near Ashgabad, Turkmenistan (**ABKT**). By recording the data in such a manner, we can look at the seismic structure of the Caspian using a variety of techniques. For example, the teleseismic body-wave recordings allow us to determine the receiver functions at each site, which can be inverted for crustal structure beneath the seismograph site. The existence of the hypothesized 'oceanic' crust beneath the Turkmenian Lowlands to the east of the south Caspian Basin should provide large converted phases, which will be easy to distinguish in the receiver function signals. Preliminary models for the crust and upper mantle structure from analysis of the teleseismic receiver function data show evidence of large sediment thicknesses beneath the southwest Caspian and a high velocity mid- to lower crustal layer beneath the Turkmenian Lowlands. Continuous data recording allows us to record teleseismic S-waves and surface waves which are more difficult to record when operating data loggers in the triggered mode. We can measure shear wave splitting which can be used to determine mantle anisotropy. The seismograph pairs are laid in such a manner that we can measure two station phase velocities for several great circle paths crossing the Caspian Basin and use these results to determine the average crust and upper mantle shear wave structure of the region. The abundant regional seismicity allows us to measure higher frequency single station phase velocities for many paths crossing the south Caspian Basin and potentially determine the three dimensional variations in the structure. From a seismic discrimination/verification point of view, this region is important because there are a number of countries in the Middle East which have a possible nuclear capability. Seismic monitoring stations for these countries are now located in the Former Soviet Union. The **Lg** phase, proven to be an effective discrimination/yield estimation phase, does not propagate across the Caspian thus preventing or at least greatly reducing its use. A better knowledge of the Caspian structure and its effect on regional seismic wave propagation will significantly improve seismic monitor capability for this and the surrounding region

DATABASE. Two years of the experiment gave more than **20 Gygabytes** of waveform data. The archive is created at the SYNAPSE Science Center on EXABYTE tapes, and serves as a mirror of the one at Cambridge University. The CSN database at the SSC is under construction, and will be populated by **CSN** data during a year or so.

DATA PROCESSING and RECEIVER FUNCTION ANALYSIS. Presently two groups of scientists - at the Cambridge University and at the SYNAPSE Science Center - work on the **CSN** data processing. First, all raw station data files are permanently archived to tape. Secondly, the data is converted into **SEGY** format, plotted by Julian day, and most events are identified using the PDE Bulletins. Third, individual events are converted into **SAC** format and event file headers are updated with appropriate source and station information. In this analysis, we examine all **CSN** teleseismic data as well as teleseismic data recorded at **IRIS** station **ABKT**.

In the first 30-60 seconds following the direct teleseismic P-wave, **P** to **S** converted and multiply reflected and converted phases (**Ps** phases) are generated by the interaction of the P-wave and the receiver structure. We use the *source equalization technique* of Langston (1979) with the modification of Ammon (1991) to isolate these Ps phases. Receiver functions are binned by common azimuth and epicentral distance and stacked if available. Shown in this poster are radial and tangential receiver functions for stations **KRV, NBD, KAT** and **LNK**, as well as for nearby **IRIS** station **ABKT**.

The response at each station is examined in terms of a 1-D or 2-D receiver structure using the techniques discussed in Langston (1977), (1979), Owens et al. (1984), Owens and Crosson (1988) and Ammon et al. (1990). To determine a 1-D model we employ the inversion procedure of Ammon et al. (1990). In this method, the radial receiver function is linearized in a Taylor series about a starting model. Each model layer is perturbed and a waveform derivative is determined for each perturbation. The difference between the model synthetic receiver function and the observed data, with a side constraint of model smoothness, is then minimized. The solution model synthetics that do not fit the most coherent phases in the data are discarded, and the remaining models represent the velocity structure. For stations **KRV** and **NBD** we show preliminary modeling results of the underlying crust and upper-most mantle velocity structure.

True amplitude receiver functions (*Rftns*) are obtained from each stations teleseismic data using the source equalization technique of Langston (1979) with the modification of Ammon (1991). Shown above is an example 'high-quality' broadband source time function teleseism recorded at station **KRV**, the radial component *Rftns* (.eqr) computed from it and the associated averaging functions. The spectral division of the horizontal components by the vertical components is computed to include frequencies up to 0.35 Hz ($a=1.0$) and using a suite of water level parameters ranging from 0.0 to 0.1 percent of the maximum peak spectral amplitude of the vertical component. The waterlevel parameter avoids numerical instabilities by division with very small numbers. Clearly present in the radial data are prominent P-SV arrivals (**Ps**) between 4-12 seconds after the direct P-wave arrival. The effect of the waterlevel is minor until **krv.01.eqr** and processing noise with values greater than 0.01 are easily observed by the averaging function's departure from an ideal gaussian pulse. We model in detail only the most stable receiver functions such as the one illustrated above, in order to avoid the deleterious effects of processing band-limited data. However, in order to examine the response as a function of azimuth, we also show *Rftns* that have an associated averaging function similar to **krv.1.eqr**.

When possible, *Rftns* from a common source region are stacked and the variance of the stacked data is used to compute +/- 1 standard deviation (*STD*) bounds. These bounds are used to constrain possible model synthetic *Rftns* that fit the **Ps** phases present in the data. The radial response examined in terms of a 1-D and 2-D receiver structure using the techniques of Langston (1977), Langston (1979), Owens et al. (1984), Owens et al. (1988) and Ammon et al. (1990).

To determine a 1-D estimate of velocity structure we employ the inversion procedure of Ammon et al. (1990). In this method the radial *Rftn* is linearized in a Taylor series about an initial model. Initial models are parameterized from previous work and/or by trial and error forward modeling.

This initial model is then randomly perturbed into 24 different starting models, each of which are inverted separately. Within each inversion, each model layer is perturbed and a waveform derivative is determined for each perturbation. In an iterative process the L2 norm between the model synthetic Rftn and the data, with a side constraint of model smoothness is then minimized. All solution model synthetics that do not fit Ps phases in the data within ± 1 *STD* are discarded. The remaining solutions represent 1-D estimates of the receiver structure. Shown below each station's radial and tangential receiver functions are the range of starting models, solution models and synthetic waveform fits to the data. Based on our experience with modeling this data, we believe the range of starting models shown adequately covers the range of possible velocity profiles at each station.

Common to all south Caspian basin data is a prominent delay of the first pulse on the radial receiver functions w.r.t. the direct P-wave arrival on the vertical component. This delay in all cases is matched with a relatively lower velocity shallow crust 2.5-3.5 km/s, compared with station **ABKT** located 400 km east of the basin, which shows no delay and does not include a low velocity shallow crustal structure.

Station **NBD** is located just outside the previously reported sub-surface extend to 'ocean-like' crust shown in Figure 4. This station shows an anomalous high velocity 'layer' with an average velocity of 7.2 km/s. This layer is the most significant model feature, and direct comparison between the radial and tangential components indicates a relatively low level of scattering (compare for example the level of scattering at station **KAT**). Therefore it is difficult to attribute this model feature as an artifact of off-azimuth energy.

Another intriguing observation can be made by comparing the relatively simple **ABKT** solutions to the **NBD** results. Both models include a step in velocity at around 20 km depth. Beneath this feature, the lower crust beneath **ABKT** is relatively constant, while the **NBD** results show a gradational lower crust.

The results at **KRV** and **LNK** are different compared to all other stations, however, an upper-mantle velocity of 8.0 km/s is consistent beneath **NBD** and although significantly deeper, beneath **LNK**. In comparison with previously reported **Pn** velocities across the south Caspian basin our results are in agreement. We observe a higher velocity upper-mantle (8.2 km/s) beneath station **ABKT**.

As more data is collected, we may be able to develop a more complete picture of the velocity structure beneath station **KAT**, as well as improve the azimuthal coverage at all stations. Our next task is to analyze the dispersion characteristics of fundamental and higher order surface wave modes of common great-circle paths inbetween these stations. An example of the kind of features in the surface wave train is shown, but not discussed in any detail. Both surface waves and receiver functions are primarily sensitive to S-wave velocity. A comparison of the results from both tasks should provide the information necessary to understand the nature of the crust and upper mantle across the south Caspian basin and surrounding regions.

Epicer locations are determined routinely in order to data collection. The process includes Wide Area Networking in terms of updating local SSC databases with fresh information from the IRIS DMC, as well as from several other seismological sources available via Internet. The work includes event association with **HDF** and **PDE** catalogues, local and regional events location, and creation of epicenter map. For this purpose we use a package *SNDA (Seismic Network Data Analysis)*, developed by the SSC, *GEOBASE Geographic Information System* by **Lamony Doherty Geological Observatory**, *MAP Geographic System* and *Seismic Analysis Code, SAC* by **Lawrence Livermore National Lab.**, and a number of software products distributed by **IRIS**

Consortium. As soon as the database of the regional events will be completed at the SSC, we will use several advanced techniques, tested on another sets of data. For example, we expect satisfactory results using *artificial neural networks* for depth determination and wave field animation. This modeling will require results on receiver function analysis.

Historical Seismogram Processing. Another part of the Caspian study is re-interpretation of old recordings of Deep Seismic Sounding (DSS) experiments. For the Caspian there are many paper records of DSS data, created during the marine experiment of the year 1956. Totally there were 2500 km of the profiles, located mainly in the Central Caspian and towards south. (**Profiles map**) The area covered by the profiles is overlapped by the area of seismic waves paths between the Turkmenian and Azerbaijanian recording sites. Using such data may improve seismic models which are to be created after processing the appropriate amount of data. There are archives of paper records in Russia and Azerbaijan, which are precious for science and tend to be corrupted by time because of natural decay. For this purpose **DGS** software package (**automated digitizing software for scanned images**) for SUN Workstations (SunOS, OpenWindows) was developed at the SSC. The database and an archive of digital waveforms of old DSS is under construction at the SSC Local Area Network equipped with SUN Workstations and PCs working under UNIX. Outside users will have an access to the database via Internet using our **WWW server www.synapse.ru**.

PROPOSED: Wide Angle Experiment. We have also initiated a new integrated seismic study of the Alpine foldbelt and south Caspian Basin using *normal incidence and wide-angle seismic data*. Because the foldbelt continue orthogonally across the Caspian Sea, it is possible to conduct a seismic acquisition program over the Alpine-Himalayan belt in the marine environment along with the advantages in cost and quality of data that marine profiling entails. The normal incidence lines will traverse from continental crust north of the foldbelt, across the foldbelt itself, across the 'paleo-continent-ocean' boundary, and penetrate southward into the interior of the south Caspian Basin and the 'ocean-like' crust zone. We propose a set of parallel dip (e.g., roughly north-south) and crossing strike lines (roughly east-west) in order to cover the principal lithospheric elements beneath the Caspian Sea. By deploying land seismometers adjacent to the sea shore, and possible ocean-bottom seismometers at sea, we shall obtain detailed compressional and shear wave seismic velocity information which will help constrain the information from the reflection profiles. The large airgun array used for the reflection profile will also provide a seismic source for wide-angle recordings.

Acknowledgments. The success of the CSN experiment was achieved because of great job done by SSC senior staff scientist **Vasily Kiselevich** and **Steve Mangino** from Bullard Lab. on array operation and data collection/processing. The help of Andrey Rasskazov on hardware support, Alexey Chulkov on data processing, and Eugeny Kapitchnikov on paper/pictures preparation is also significant. We also thank Dr. Batyr Karryev for his contribution to this research.

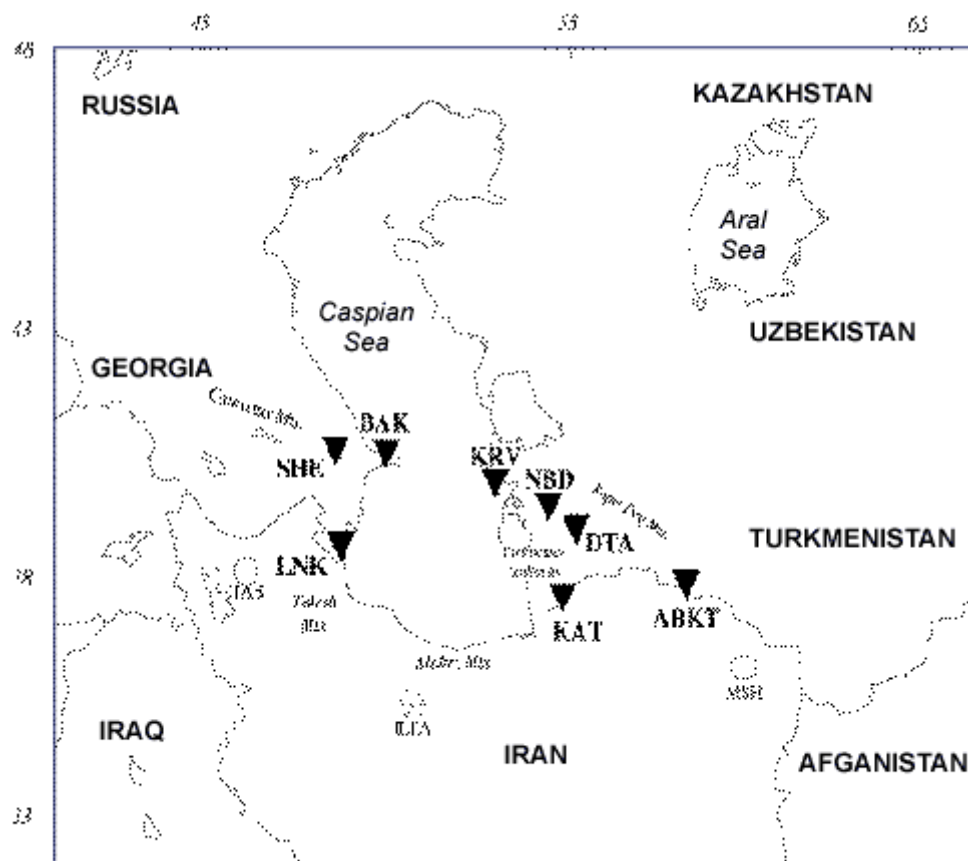
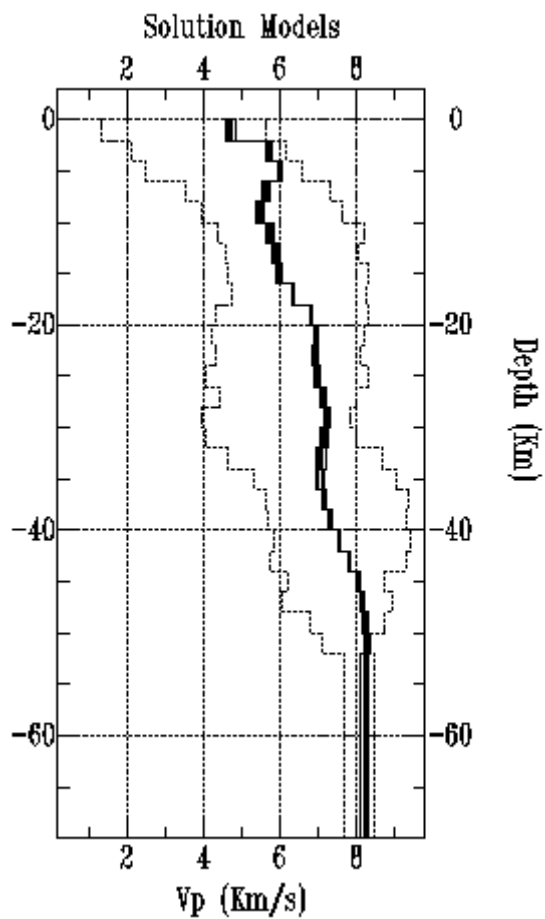
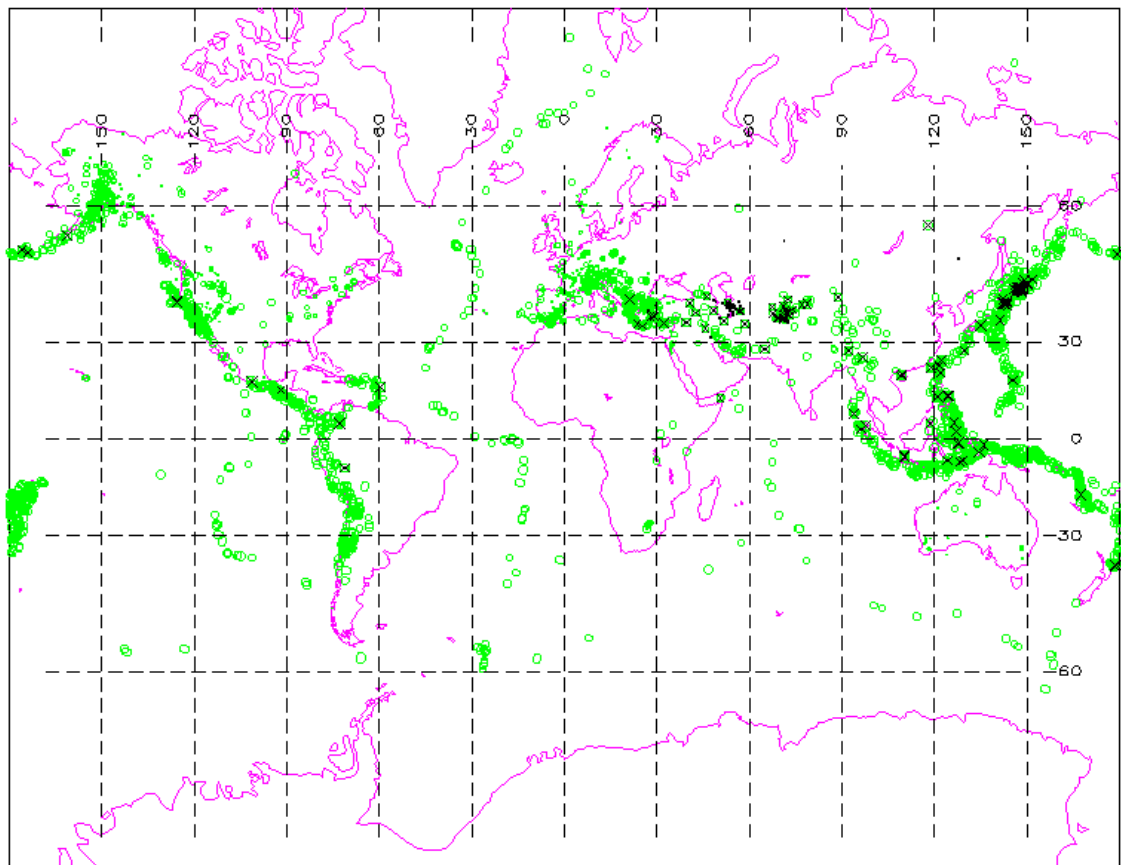


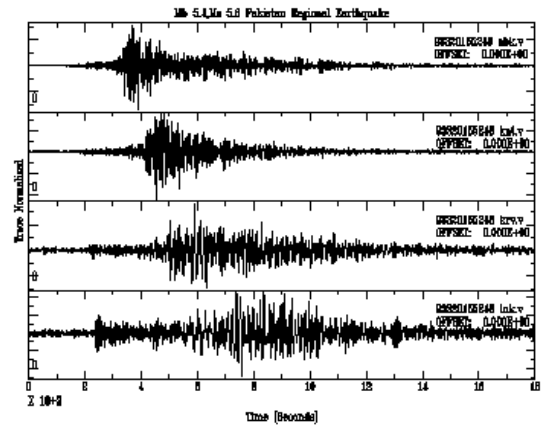
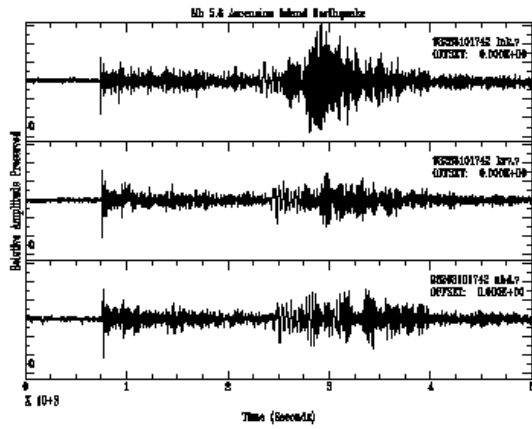
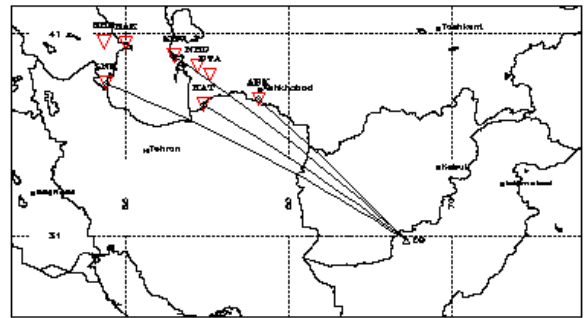
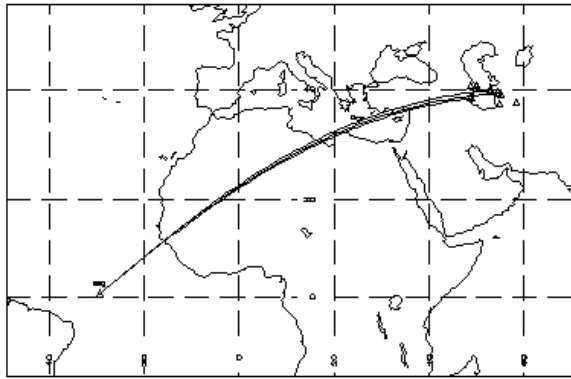
Fig.1



PROJECTION: MERCATOR, CENTER: 0.00 0.00 0.0
WINDOW ANGLES 180.0000 180.0000 80.0000 80.0000

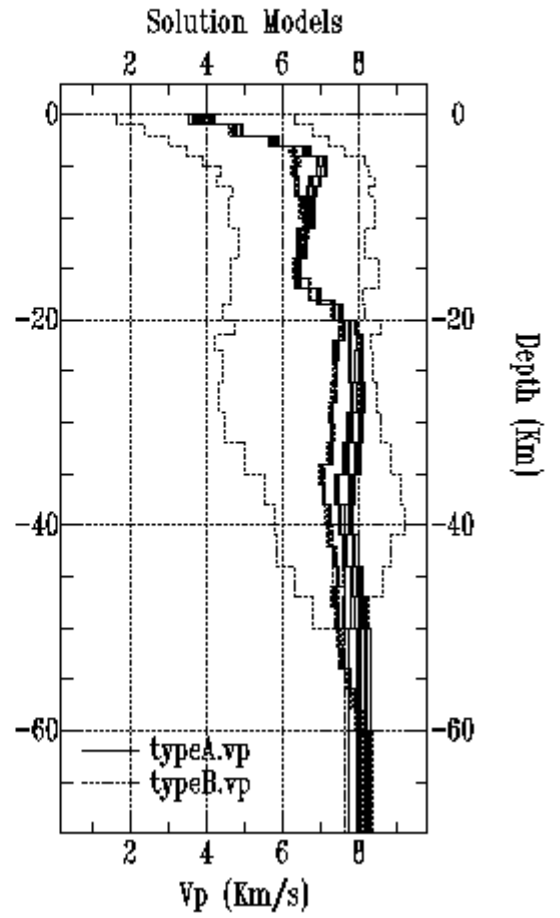
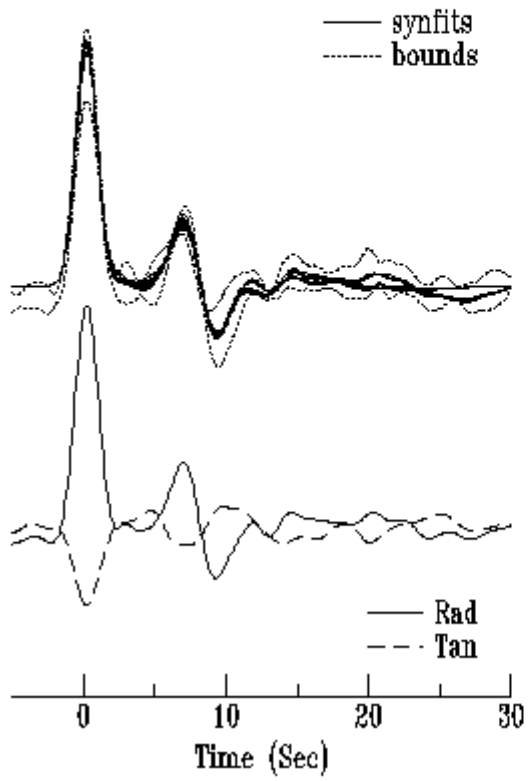
SURFACE WAVES BLOCADE BY THE SOUTHERN CASPIAN BASIN

Asension Island EQ Pakistan EQ



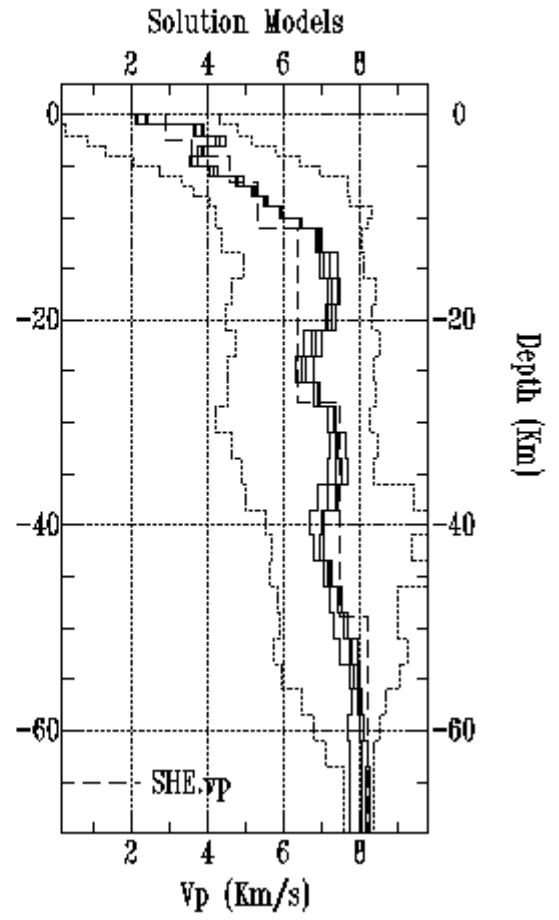
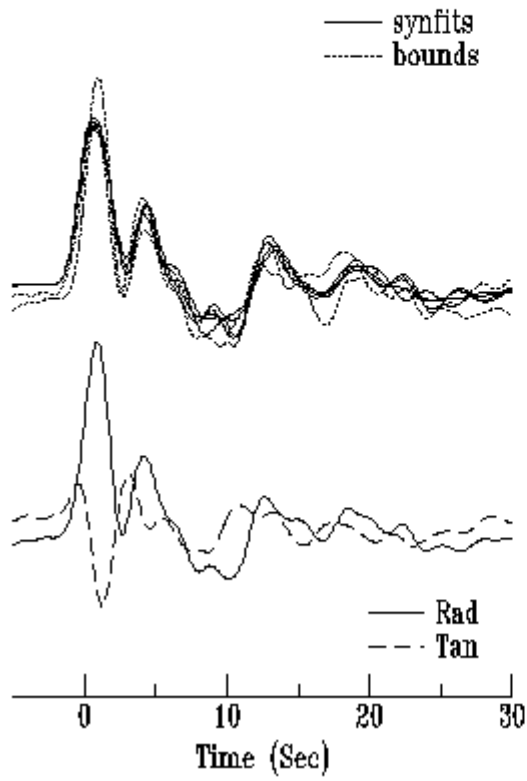
STATION KRV

Synthetic Rftns vs +/- 1 STD (top)
Radial vs Tangential Rftn (bottom)



STATION LNK

Synthetic Rftns vs ± 1 STD (top)
Radial vs Tangential Rftn (bottom)



STATION NBD

Synthetic Rftns vs Data (top)
Radial vs Tangential Rftn (bottom)

